Journal of Microbiological Methods 159 (2019) 81–90

Contents lists available at ScienceDirect

Journal of Microbiological Methods

journal homepage: www.elsevier.com/locate/jmicmeth

Settling velocity and size distribution measurement of anaerobic granular sludge using microscopic image analysis

Fasil A. Tassew*, Wenche Hennie Bergland, Carlos Dinamarca, Rune Bakke

Department of Process, Energy and Environmental Technology, University of South-Eastern Norway, Kjølnes ring 56, NO 3918 Porsgrunn, Norway

ARTICLE INFO

Keywords:
Settling velocity
Anaerobic granule
Size distribution
Biogas reactor
Image analysis
Shape factor

ABSTRACT

Settling velocity and size distribution of anaerobic granular sludge samples were studied using microscopic image analysis and settling column experiments. Five granule samples were considered in this study. Three samples were collected at the Top, Middle and Bottom sections of a lab scale upflow anaerobic sludge bed reactor (UASB). Two other granule samples were obtained from industries. This paper aims to establish a method that uses microscopic image analysis and shape factor as a tool to determine the size distribution and settling velocity of anaerobic granules. Image analysis technique was used to calculate the shape factor and equivalent diameter of granules. The equivalent diameter was then used to calculate the theoretical settling velocities based on Allen's formula and estimate size distributions.

The results showed that there was a good agreement between the theoretical and experimental mean settling velocity values. Both measured and calculated settling velocities increased with increasing Reynolds number (*Re*). However, the agreement between measured and calculated values was found to be weaker at higher *Re* values. Size distribution analyses of the granules have revealed that there was significant difference in the size distribution of granule samples collected at different heights of the lab scale reactor. Overall, granules from the bottom section of the reactor had larger diameter, settling velocity and shape factor than those at the middle and top section granules. Whereas granules collected from the top section exhibited the smallest granular diameter, settling velocity and shape factor.

1. Introduction

Settling velocity of anaerobic granular sludge is an important characteristic of a UASB reactor. The resistance of anaerobic granules to washout and remain in the reactor is the main reason for the success of UASB systems. Several factors, ranging from fluid and flow properties to granule size and density influence the settling property of granules. Biogas production process involves a complex set of anaerobic biochemical reactions that result in the breakdown of organic compounds into smaller molecules. This process results in biomass growth (change in the granule size and density) and production of gas, which influences settleability of granules as the process progresses. As a result, it is important to monitor the settling behaviour of granules regularly. Several different methods have been used to measure settling velocity. For example, Ahn and Speece (2003) and Vlyssides et al. (2008) estimated settling velocity of granules by measuring the percentage of washed-out granules when a given up-flow velocity is applied at the bottom of granular sludge bed. Others, such as Ghangrekar et al. (2005), used a glass column to measure settling velocity based on the fraction of granules settled in a given time interval. In this article, the settling velocities of anaerobic granules were directly measured in a settling column using a high-speed camera. Microscopic image analysis was used to quantify granule perimeter, area, shape factor and equivalent diameter to estimate size distribution and theoretical settling velocity. Although there have been works that used image analysis to estimate particulate size (Thaveesri et al., 1995; Tang et al., 2011; Alves et al., 2000; Bellouti et al., 1997), the author of this article has not found studies that applied the granule shape factor method as used in the present article for the study of size distribution and settling velocity of granules from UASB reactors. A correlation of settling velocity of granules and the reactors' flow parameters such as Reynolds number (*Re*) was established.

1.1. Settling velocity

Granules settling in a liquid experience three main forces acting upon them: gravity, buoyancy and drag forces. Depending on the type of the flow regime, theoretical calculations of terminal/settling velocity

* Corresponding author.
E-mail address: fasil.a.tassew@usn.no (F.A. Tassew).

https://doi.org/10.1016/j.mimet.2019.02.013
Received 31 January 2019; Received in revised form 21 February 2019; Accepted 21 February 2019
Available online 22 February 2019

(V_t) of a granule vary. Early papers about granule settling used Stokes flow ($Re < 1$) for granule settlement calculations (Gupta and Gupta, 2005; Laguna et al., 1999). However, this may not be accurate since it has been shown that the Reynolds number of anaerobic granular sludges in typical UASB reactor conditions falls in the intermediate flow regime category (*Re* between 1 and 500). Allen's formula has been used to calculate settling velocity of granules in the intermediate flow regime [Liu et al., 2006]. It was derived by inserting the drag coefficient (C_d) equation for intermediate regimes into the general terminal velocity equation:

$$V_t = \sqrt{\frac{4g(\rho_g - \rho_f)}{3C_d\rho_f}} \quad (1)$$

$$C_d = 18.5Re^{-0.6} \quad (2)$$

$$Re = \frac{\rho_f D_g V_t}{\mu_f} \quad (3)$$

$$V_t = 0.781\left[\frac{D_g^{1.6}(\rho_g - \rho_f)}{\rho_g^{0.4}\mu_f^{0.6}}\right]^{0.714} \quad (4)$$

Where, D is diameter, ρ is density, μ is viscosity and the subscripts g and f denote granule and fluid respectively. The above equations are formulated assuming that particles are spherical in shape, hence settling velocity calculation for granules have to include a factor for the non-sphericity of the granules. The equation for terminal velocity includes a term for drag coefficient and the drag coefficient equation includes a term for Reynolds number. However, Reynolds number is calculated using terminal velocity value. This is a form of "circular equation" and has to be solved iteratively until the correct values for Re, V_t and C_d are found (Dietrich, 1982).

1.2. Granule size distribution

Size and shape of a granule along with density all but determine what the settling behavior of the granule will be. Anaerobic granules are usually assumed to be spherical with a diameter ranging from 0.5–5 mm. Granule size is one of the most important factors in UASB reactors. It has been shown that size of granules affect most aspects of a UASB reactor performance (Wu et al., 2016). The size of granules change during the course of the biogas production process due to microbial growth and decay, granular shear-off, granule-granule collision and granule-wall collisions. As a result, it is important to monitor changes in granule size regularly. Theoretically, increase in the granule size can be estimated from bacterial yield coefficient, specific substrate utilization rate and specific endogenous decay rate. See Yan and Tay (1997).

There are different granule size measurement techniques. The two most often used techniques are the gravimetric method and image analsys methods. In the gravimetric method granular sizes are calculated indirectly from settling experiments (Grotenhuis et al., 1991). Whereas in the image analysis method granule sizes are directly measured from microscopic images using image processing software. Other methods such as Laser particle size analysis (Yan and Tay, 1997) and automated image analysis (Laguna et al., 1999) are also used. In this paper, equivalent diameter of granules were calculated from the perimeter and shape factor of two-dimensional granular images. Once diameters of the granules are known, the size distribution can be expressed in various ways (number, area or volume distributions). A reporting of the mean value alone may be enough for some applications but in this paper, we decided to report the granule size distribution as a number distribution since we believe it carries more information about the size of the granules. In this method, granules are grouped into size ranges and the number of granules in each size range is counted and plotted as a number frequency versus size range plot.

1.3. Image analysis

Microscopic image analysis has been used for the determination of size and shape of granule samples. The method is suited for granules that are non-spherical because it enables different definitions of granule sizes to be used to characterize samples (eg. Equivalent diameters) Olson (2011). The accuracy of the measurement depends on several factors such as microscope calibration and the quality of the images taken. The calibration step can be carried out using a standard micrometer ruler (e.g National Institute of Standards and Technology, NIST, traceable stage micrometer). The quality of the image can be affected by granule overlap, presence of bubbles, too much or too little lighting, non-granular solid materials etc.

2. Materials and methods

During the course of this study several different methods and equipments have been used. Microscopic image analysis was used to measure equivalent diameter of granules (D_g). Equivalent diameter of granules were used for size distribution plots and also to calculate theoretical settling velocity of granules. Experimental measurement of settling velocity was also carried out and compared with the theoretical settling velocity. Factors that affect the measurement methods are also described Fig. 1.

2.1. Sample source

The main source of the granular samples is a lab scale vertical UASB reactor that has been treating centrifuged pig manure collected from storage room from a farm near Porsgrunn, Norway. It has a height of 0.85 m, internal dimater of 4.4 cm and a total volume of 1.3 L. The reactor has been operated at an organic loading rate (OLR) of 3.1 Kg/m^3d, upflow velocity of 1.75 m/h and hydraulic retention time (HRT) of

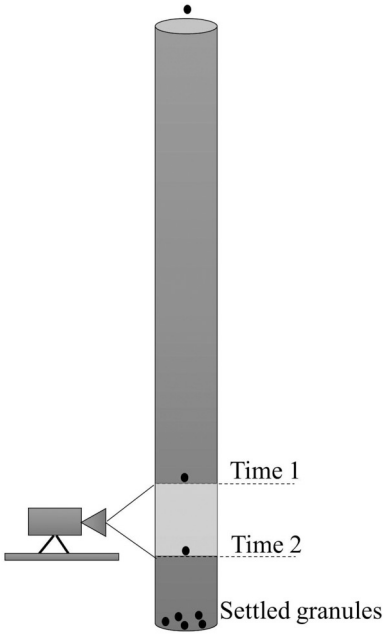

Fig. 1. A schematic diagram of settling velocity measurement set-up.

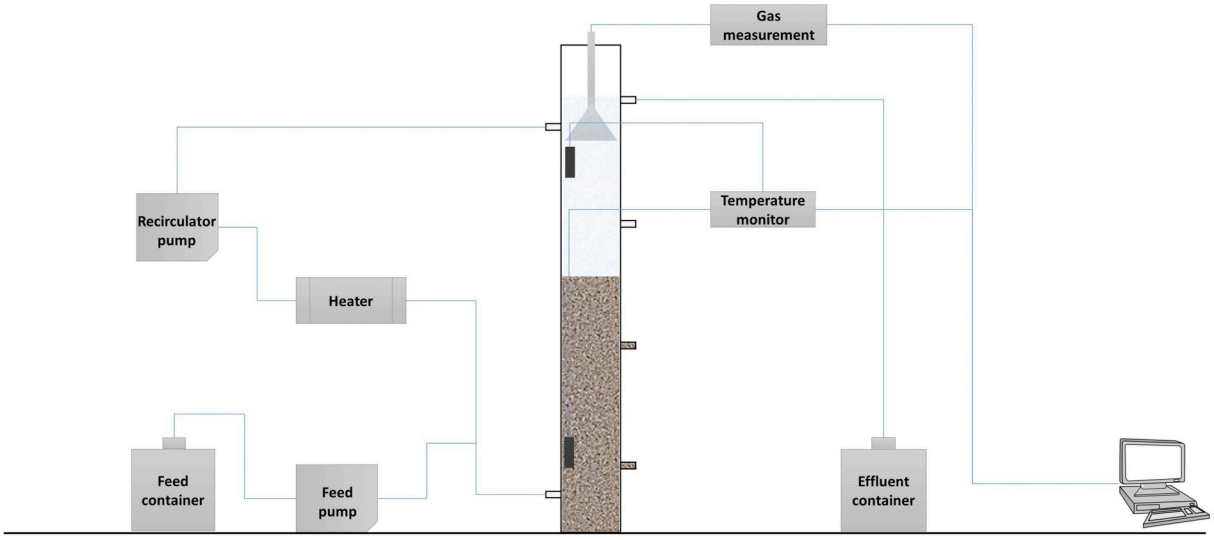

Fig. 2. A schematic diagram of lab scale UASB reactor.

Table 1
Description of anaerobic granular sludge samples. (N_{Vt} and N_{sd} are number of granules used in settling velocity and size distribution experiments respectively.)

Sample	Origin	Days in reactor	N_{Vt}	N_{sd}
Fresh	Econvert	0	200	50
Top	Top sampling portal	80	200	50
Middle	Middle sampling portal	80	200	50
Bottom	Bottom sampling portal	80	200	50
Borregaard	Full scale reactor	0	50	50

5 days at 38C. It is equipped with a heating & recirculation and feed pumps. A biogas flow meter based on volumetric flow measurement was integrated (Dinamarca and Bakke, 2009). Data from temperature sensors and gas flow measurement were collected and monitored using LabVIEW software (LabVIEW 2014 and LabVIEW 2015). Granule samples were taken from three sampling portals in the reactor: Top section, Middle section and bottom section. See Fig. 2. In addition, two other granule samples from industry were used. The first one is granule sample that has been treating wastewater from paper factory in an internal recirculation anaerobic reactor from Econvert Water & Energy, Netherlands. The other one is from Borregaard treatment plant, Norway. Granules from econvert are also used as a seeding granules for the lab scale reactor and their inclusion in the study will help in the investigation of the effect of reactor conditions on granule characteristics. The granule samples from Borregaard treatment plant are included in the study in part because upon visual inspection they appear to be comparatively flat, as opposed to spherical, than that of granule samples from the UASB reactor. The difference in size and particularly in shape would provide an opportunity to test the validity of the proposed method Table 1.

2.2. Image analysis

A calibrated Nikon microscope was used to take granular images. The images were taken in such a manner to avoid granule overlap and bubble formation. For granule samples from the lab scale UASB reactor images of up to 200 granule were taken. For Borregaard granule samples 50 images were taken. All images were preprocessed using a matlab code (MATLAB R2015a) to make them ready for size and shape measurement. Image preprocessing was done to separate adjacent granules, remove bubbles, adjust the lightening and eliminate non-granular solid materials. The perimeter, area and shape factor of granules in the preprocessed images were measured using a separate matlab code. The perimeter and area of granules were measured using built-in matlab functions whereas shape factors of the granule were measured according to the following steps: First, the code locates the centroid position of a granule, then all the distances from the centroid location to all the edge points of the granule are measured. The shape factor is then calculated as a standard deviation of all the distances from centroid location to each pixel at the edges of the image of the granule. Ideally, if a granule is spherical, then its two-dimensional image will be circular and all the distances from the centroid to the edges will be equal to its radius giving a standard deviation of zero. However, actual granules exhibit shapes that are different from spherical. As the granule shape becomes more and more irregular, the shape factor value increases. Fig. 3 illustrates the shape factor calculation scheme: The shape factor (SF) of a given granule is calculated by using the standard deviation equation used in matlab. It is given as:

$$SF = \sqrt{\frac{1}{N-1}\sum_{i=1}^{N} |A_i - A_{mean}|^2} \quad (5)$$

$$A_{mean} = \frac{1}{N}\sum_{i=1}^{N} A_i \quad (6)$$

Where: A_i is an individual distance from a centroid of a granule to its edge, A_{mean} is average of all distances from centroid to perimeter edges and N is the number of distances measured.

Calibration of the microscope was carried out for each magnification and zooming level using a standard micrometer ruler. The

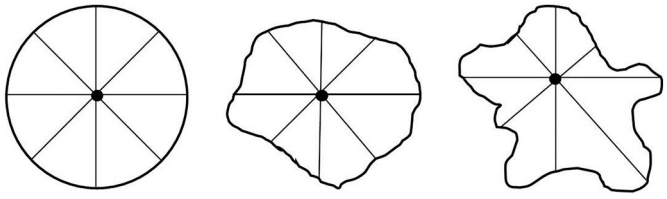

Fig. 3. Illustration of shape factor measurement.

calibration data was then incorporated in to Matlab code so that granule size results can be converted from pixels to millimetres.

2.3. Equivalent diameter

There are several methods to calculate equivalent diameter for non-spherical particles such as: Volume equivalent sphere diameter, surface equivalent sphere diameter, projected area diameter etc. One of these methods is based on the circularity of a particle. Circularity (C) of a particle is a measure of similarity of its shape to that of a perfect circle (Olson, 2011). It uses both the area (S_A) and perimeter (P) of the particle to estimate its circularity. ISO 9276:2008(en) is a standard from the international organization for standardization that deals with the quantitative representation of particle shape and morphology. In section six of the standard, the circularity of a particle is defined as:

$$C = \sqrt{\frac{4\pi S_A}{P^2}} \tag{7}$$

Podczeck and Newton (1995) suggested an equation for measurement of surface texture/roughness (S_r) based on the perimeter and mean of the distances from the centroid to the edge of the perimeter (A_{mean}).

$$S_r = \frac{2\pi A_{mean}}{P} \tag{8}$$

In this paper, a modified form of the above equation is used to estimate the equivalent granule diameter (D_g). It is based on granule perimeter (P) and its shape factor (SF):

$$D_g = \frac{P}{\pi}\left[\frac{1}{1+\sqrt{\frac{2\pi SF}{P}}}\right] \tag{9}$$

Bouwman et al. (2004) studied different types of shape factors used to analyse the shape of granules. The shape factors studied range from those based on aspect ratio of granular images to those based on Stoke's shape factor. They also studied radial shape factor that estimates the center of gravity of granule images to determine shape factor. Eq. (9) is based on a similar concept and can be considered as a modified form of the radial shape factor. For spherical granules Eq. (9) is equal to P/π. However, irregular shaped granules have larger perimeters than granules of similar projected area. For example, a circle and a square with 1 m^2 area will have a perimeter of ≈3.54 m and 4 m respectively. The term in the bracket in Eq. (9) accounts for the overestimation of diameter of irregularly shaped granules.

2.4. Settling velocity

Settling velocity of individual granules were measured using a 1.5 m glass column using a high-speed digital camera followed by image analysis. The settling column was made of a transparent glass and it is 1.5 m in height and 4.5 cm in diameter. The column was set up vertically and filled with tap water at room temperature. Individual granules were released carefully in the middle of the top of the water surface. Then the granules were allowed to settle. At 1.35 m from the top of the glass column, a tape with a known length (0.037 m) was attached in such a way to cover half the circumference of the glass column. Granules will accelerate until they attain a constant settling velocity. As a result, the measurement of settling velocity should be carried out after constant velocity is achieved. The settling column should be long enough to allow the granules to reach their constant settling velocities. Preliminary tests indicated that, granules of 0.5–5 mm diameter and 1050–1090 Kg/m^3 density travel around 0.5–1 m before attaining constant velocities. So, a distance of 1.35 m was assumed to be enough length for the granules to reach their settling velocities. Since the granules are black in color a contrasting white tape was used. A high-speed digital camera was placed in front of the tape. The camera recording was set to 50 frames per second (fps) for a precise resolution of time and distance when the granules cross the boundaries of the attached tape. Most of the granules were able to settle vertically without touching the column walls. Granules that touched or collided with the column surface were excluded from the measurement. Similarly, granules that settled without colliding with the wall but crossed the tape boundaries at non-vertical lines were excluded. To avoid hindered settling and influence due to possible particle collisions, individual granules were not allowed to settle in close proximity. Besides the parameters expressed in the previous equations, the settling velocity of granules can also be affected by factors such as shape, surface roughness, wall effect etc. Dietrich (1982) studied the effect of particle shape, roundedness and surface roughness, among others, on settling velocity. It was pointed out that when non-spherical particles settle they tend to orient their largest projected area against the direction of the flow (settling). This leads to a larger drag force and a decrease in the settling velocity of the particle compared to an equivalent particle with spherical shape. Similarly, surface roughness also leads to lower settling velocity by increasing the drag force, however, its effect is not thought to be as significant as particle shape Table 2.

Table 2
Theoretical and experimental settling velocity and density of granules.

Granule	ρ(Kg/m^3)	Measured V_t	Calculated V_t
Fresh	1070	63.14	66.97
Top	1075	45.02	45.93
Middle	1075	58.9	56.57
Bottom	1070	68.49	63.13
Borregaard	1015	61.95	58.54

2.5. Wall effect

Particles settling in a viscous fluid within a confined wall experience slower settling velocities than those of “free settling” particles (Chhabra et al., 2003). This is due to the wall-effect (f_w). Wall effect is usually defined as the ratio of terminal velocities of a particle settling in a confined wall (V_t) and a particle settling in a wall of infinite internal diameter (V_∞). A number of papers have been published that deals with the estimation of the wall effect (Ataide et al., 1999; Zhang et al., 2016; Arsenijević et al., 2010). In those papers, β, a ratio of particle diameter (in this case, D_g) and diameter of the wall (D_{pipe}) was used as a starting point to estimate wall effect. Ataide et al. (1999) studied the wall effect over wide ranges of *Re* and *b* values and proposed Eq. (10) for theoretical estimation of wall effect and found a good fit (R^2 = 0.96) between experimental and predicted values. In this paper, wall effect was estimated based on the equation suggested for Re values between 0.38 and 310 and β values between zero and 0.55. This is well within the samples range of *Re* and β values.

$$f_w = \frac{V_t}{V_\infty} = \frac{10}{1 + A\mathrm{Re}^B} \tag{10}$$

Where, $\beta = D_g/D_{pipe}$, $A = 8.91e^{2.79\beta}$ and $B = (1.17 \times 10^{-3}) - (0.281\beta)$

The terminal velocity calculated without considering the influence of the wall effect, such as the V_t in Eq. (4) is in fact V_∞. The terminal velocity that takes the wall effect into account is given in Eq. (11).

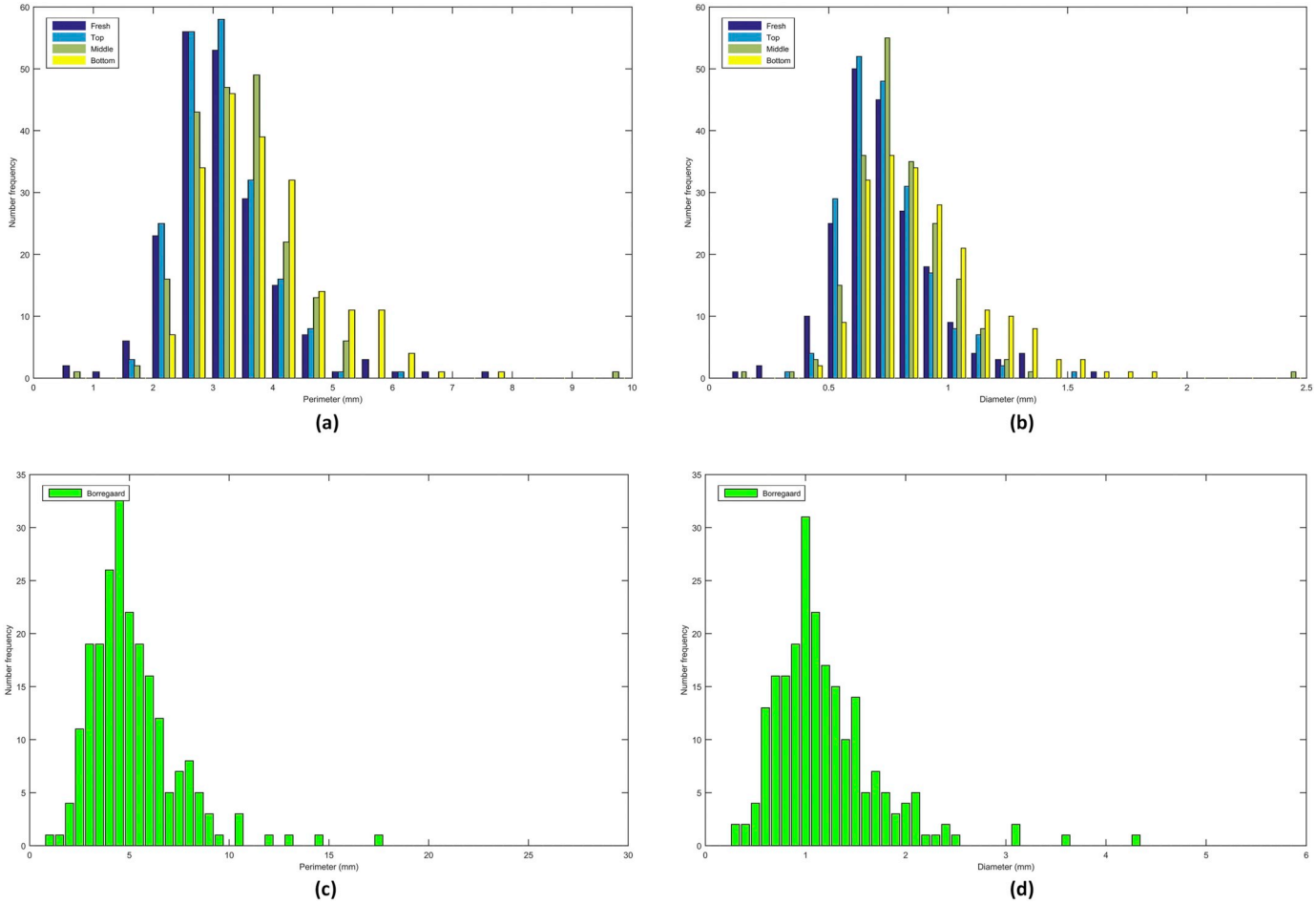

Fig. 4. Size distribution of granules based on perimeter and diameter: a& b: granules from lab reactor and c& d: granules from Borregaard reactor.

$$V_t = 0.781 f_w \left[\frac{D_g^{1.6}(\rho_g - \rho_f)}{\rho_g^{0.4}\mu_f^{0.6}} \right]^{0.714} \quad (11)$$

2.6. Granule density

Density of the granule samples were measured using a pycnometer. The pycnometer method have been used to determine density of solid particles, powders, granules, and dispersions Pol (1989) and Vlyssides et al. (2008) have used a method adapted from Mahling (1965). In this method, the weights of granules and distilled water at a given temperature are measured and then the granule density is calculated as follows:

$$\rho_g = (\rho_w - \rho_a)\frac{M_2 - M_1}{(M_2 - M_1) + (M_4 - M_3)} + \rho_a \quad (12)$$

Where, M_1: Weight of dry pycnometer, M_2: Weight of dry pycnometer and granules, M_3: Weight of dry Pycnometer, granules and water, M_4: Weight of pycnometer and water, ρ_g: density of granule, ρ_w: density of water and ρ_a: density of air.

3. Results

3.1. Granule size distribution

The size distribution graphs were given as a Perimeter plot, which was obtained directly from image measurement and as an equivalent diameter plot, which was based on Eq. (9). Size distribution measurement for the sample from Borregaard plant involved a different number of granules than the rest of the samples. As a result, it was decided to provide the result in a separate plot. The results are shown in Fig. 4.

The result showed that there is a clear variation in the size distribution along the height of the lab scale UASB reactor. Granules from the top section of the reactor have an average and median perimeter of 2.7 mm and 2.61 mm respectively whereas the average and median equivalent diameters are 0.65 mm and 0.63 mm respectively. For the middle section granules the average and median perimeters were 2.94 mm and 2.84 mm and the average and median equivalent diameters were 0.71 mm and 0.68 mm. This indicates that the overall size of the granules increase towards the bottom of the reactor. This pattern is even more clear when one looks at the result from the the bottom section granules. At average and median diameters of 0.81 mm and 0.75 mm the bottom section is dominated by the biggest granules of the reactor. Laguna et al. (1999) also reported that the biggest granules dominate the bottom section of a reactor they studied. If one considers granules lower than 0.5 mm equivalent diameter, the fresh granules dominate followed by the top section granules. Overall the Fresh and Top section granules show similar size distribution. Size distribution within each sample group also varies. Top section granules are comparatively more uniform in size than that of middle and bottom section granules. The same is true when it comes to shape analysis. Granules from the top section are more spherical (lower shape factor value) than their lower section counterparts. In most of the size frequency groups,

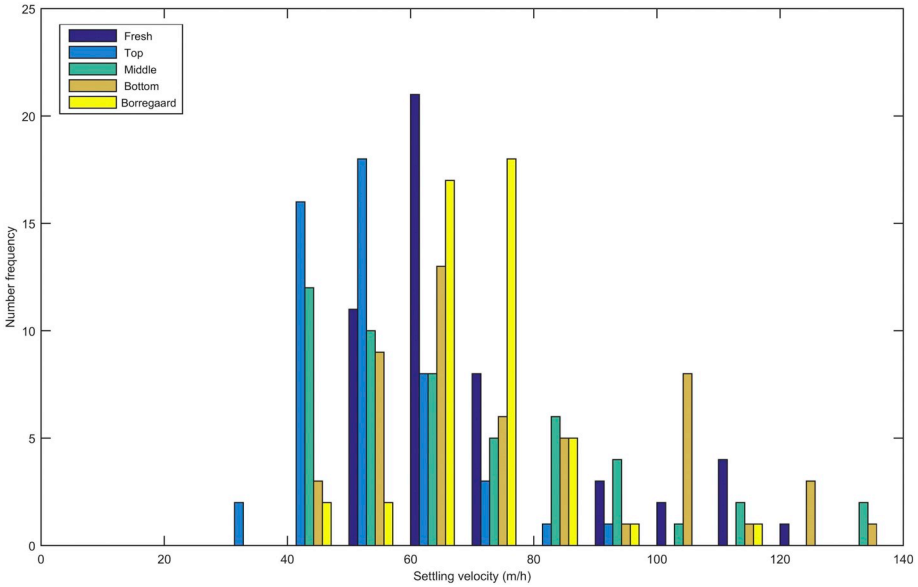

Fig. 5. Settling velocity distribution of granules.

the Fresh granules are the smallest compared to the Top, Middle and Bottom section granules. In addition, the median and the average diameters are also the smallest. This is expected because, unlike the Fresh granules, the Top, Middle and Bottom section granules undergo biomass growth in the reactor over a period of 80 days. As a result, their size increases. Granules from the Borregaard sample are generally bigger than the granules from the UASB reactor. The average and median sizes are 11.01 mm and 10.95 mm for perimeter and 2.65 mm and 2.66 mm for equivalent diameter. There is also a higher size variation of granules in the Borregaard sample than the samples from the UASB reactor. The standard deviation of Borregaard granule diameters is 0.77 mm where as all the other granules samples have a standard deviation below 0.25 mm. The average shape factor of Borregaard granules is 0.19 mm which is much more than the shape factors for the samples from the lab scale reactor (0.05 mm, 0.044 mm, 0.051 mm and 0.057 mm for fresh, top Middle and bottom section samples respectively). This suggests that the Borregaard granules are much less spherical than the other granule samples. This was also confirmed by simple visual inspection Fig. 5Fig. 6 and Fig. 7.

3.2. Settling velocity

The settling velocity of 50 individual granules from each sample group were measured and compared with theoretical calculations for settling velocity. The results are reported as a mean settling velocity. In addition, the agreement between theoretical and experimental values were compared based on Reynolds number values. The mean settling velocity of the granules is given in Table 2, whereas, comparison of theoretical and experimental settling velocities are given in Fig. 6. Median and Standard deviation values are given in Table 3.

Settling velocity of samples were measured and compared with theoretical values. The results showed good agreement between the theoretical and experimental values. The theoretical and experimental mean settling velocities of each sample is less than relative error of 8.5%. Generally, both the measured and calculated values increase with increasing *Re* for all samples. However, the agreement between the measured and calculated values become weaker at higher *Re* values. Percentage relative error was calculated for each measurement and sorted from the lowest to the highest. Then the average *Re* of those below the median relative error was calculated and compared with those that have relative errors above the median value. For the Fresh sample the average *Re* below and above the median relative errors are 15.01 & 33.85. Those values are 10.63 & 10.65 for the Top section, 13.74 & 17.80 for Middle section, 16.98 & 22.82 for Bottom section and 47.72 & 48.19 for Borregaard samples respectively.

4. Discussion

4.1. Granule size distribution

The granule size distribution result showed that there is variation in granule size from the top to the bottom section. Generally, granule size increases from top section to the bottom section. The variation in granule size along the reactors height may be simply due to stratification of granules based on their density variation but this was not supported by density measurement and the bottom section granules have similar density with that of the fresh granules and in-fact have marginally lower density than those of the middle and top section granules. Yan and Tay (1997) found that the bottom section of a reactor is also the location where the biggest granules dominate. In addition, they observed that granule formation and growth mainly takes place at the bottom section and theorized that the existence of bigger granules in the bottom section is not only due to stratification but also because of the higher substrate loading around the bottom section compared to the rest of the reactor sections. Laguna et al. (1999) noted that not only do bigger granules tend to be found at the bottom of a reactor but the proportion of bigger granules in each section increases over time. This was observed in the UASB reactor.

Fresh granules (0 days in the reactor) have the smallest granules in most of the size groups in all samples which were in the reactor for 80 days (see Fig. 4).

Fresh granules and granules from the top section of the reactor showed smaller shape factor values than granules from the middle and bottom sections. As a result, Fresh and top section granules can be considered “more spherical”. This may be due to the difference in the growth of microbes across the reactor height. Due to easier substrate

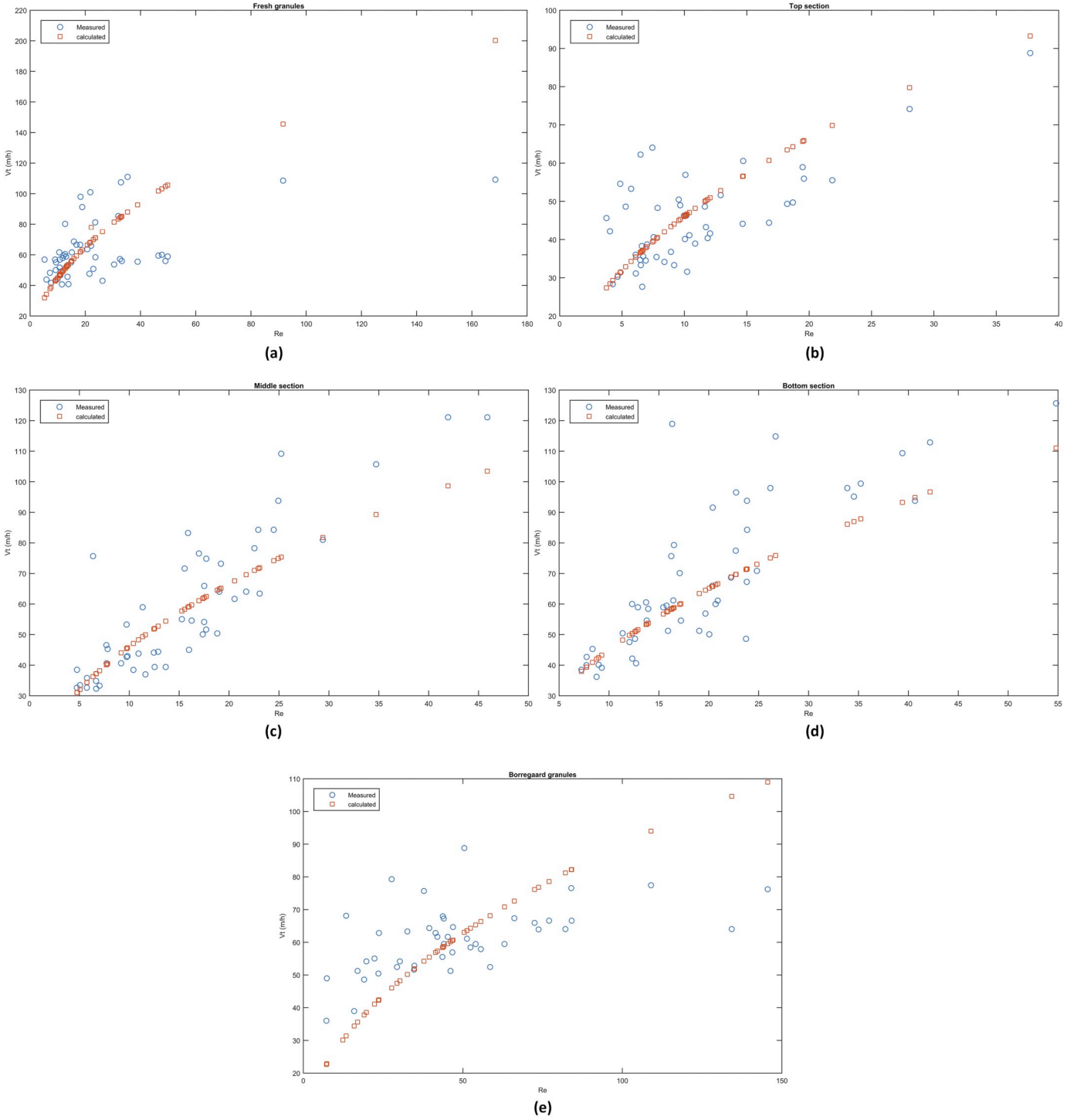

Fig. 6. Comparison of theoretical and experimental terminal velocity of granules with respect to *Re*. (a: Fresh b: Top c: Middle d: Bottom e: Borregaard).

access, bottom and middle section granules grow larger than the top section granules. The growth of granules across a granule surface may be uneven and contributes to the higher shape factor. Moy et al. (2002) found evidence of a link between high organic loading rate and formation of irregular shaped granules in their study on effect of loading rate on physical properties of aerobic granules. Higher hydrodynamic activity near the feed inlet at the bottom section may also contribute to granule shear-off. Since the lab scale reactor uses an intermittent feed pattern, the abrupt change in the loading rate may have affected the strength of granules at the bottom. This is corroborated by Alpenaar and granular Sludge (1994) who found evidence that abrupt changes in the loading rate affects the mechanical strength of granules. At the top section granule growth is limited due to poor substrate access and also lower hydrodynamic shear-off.

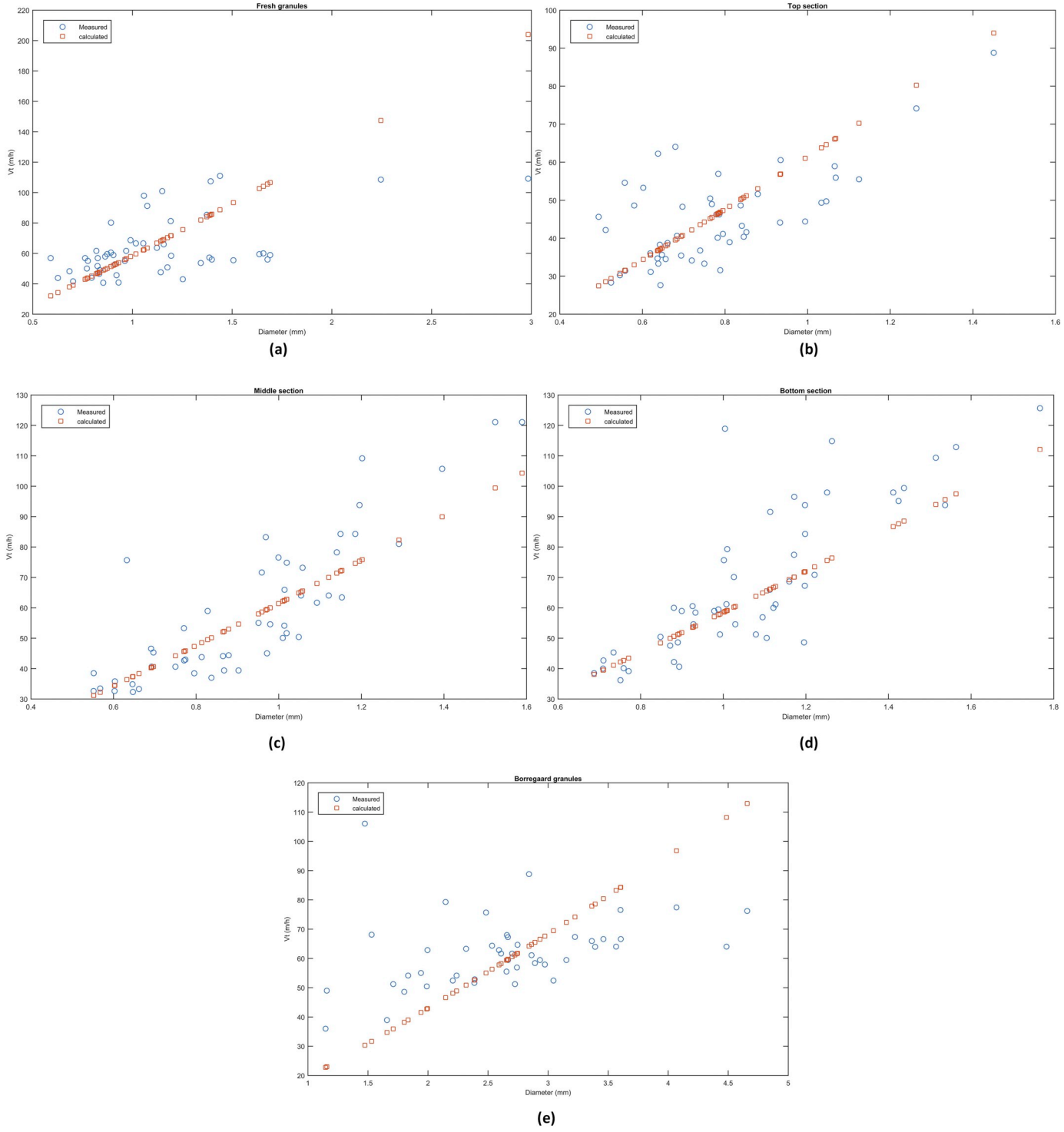

Fig. 7. Comparison of theoretical and experimental terminal velocity of granules with respect to granule size. (a:Fresh b: Top c: Middle d: Bottom e: Borregaard).

Borregaard granules showed the highest size variation and shape factor of all the samples. The reason may be related to the mechanical strength of the Borregaard granules. Borregaard granules were broad and flat in shape. Even though no mechanical strength test was done, it was observed that the granules easily break apart during microscopic size measurement and settling velocity measurement. The weak mechanical strength may allow different sized chunks of granules to break-off and this increases the variation in size and shape factor.

4.2. Settling velocity

The mean settling velocity of granule samples except for the top section granules are in the range of typical anaerobic granule settling velocities. Pol et al. (2004) reported that anaerobic granules usually have settling velocities of approximately 60 m/h. The mean settling velocities of the samples in this study are close to that value. However, at 45.02 m/h, top section granules have significantly lower mean

Table 3
Median and standard deviation of measured and calculated settling velocities in m/h.

Sample	Test	Median	Standard deviation
Fresh	Measured	57.58	19.04
	Calculated	58.47	29.31
Top	Measured	43.25	12.02
	Calculated	44.05	13.45
Middle	Measured	52.46	23.24
	Calculated	58.01	16.77
Bottom	Measured	60.27	24.04
	Calculated	60.01	16.15
Borregaard	Measured	61.67	11.97
	Calculated	58.61	19.05

settling velocity than that of the reported value. Granules from the top section are also smaller in size than the rest of the granules in the reactor. Based on Eq. (11), it is expected that top section granules will also be the ones with the lowest settling velocity. Other studies such as, Ahn and Speece (2003) also found low settling velocities for granules in the upper section of a reactor.

Granules at the top section also have a limited access to substrates since they are located the furthest from the feed inlet. This may have restricted microbial growth while facilitating decay & granular shear-off. However, granular shear-off is likely to happen more at the bottom section where bigger granules populate, then the sheared-off and presumably smaller granules float upwards and accumulate at the top section. In a study of granular strength, Pereboom (1997) found out that methanogenic granules with bigger sizes are more likely to face abrasion and shear-off than smaller ones. This contributes to keeping the granules at the top to be relatively smaller than granules from other section and by continuation also contributes to the low settling velocity (granules may contain organisms that can apply tropism, such as in clostridia, but it is assumed not to be expressed in such granules given the strong mixing and shear forces in all efficient sludge bed reactors). The agreement between calculated and measured settling velocities showed dependence on the *Re* value. At lower Re values there was a better agreement than at higher Re value. Granules with small size also have small *Re* and as a result their measured and calculated settling velocities have better agreement than bigger granules. The best agreement between measured and calculated settling velocities is found in the top section granules, which are the smallest in size, while the worst agreement is in the Borregaard granules. Borregaard granules showed the highest relative error even at lower *Re* values. In addition to the contribution due to their relatively bigger size, the high relative error can also be explained by the effect of the shape of the granules on the measured settling velocity. Dietrich (1982) pointed out that granules that deviate from the ideal spherical shape will have surface curvatures, usually next to the maximum projected area, that are more curved than if the granules were spherical. This increases the drag coefficient and leads to lower settling velocity than that of a spherical granule of the same size. Borregaard granules were, in general, broad and flat and their shape factor measurement was the highest of all the samples. In addition, being broad and flat makes them susceptible to shear-off and rotation during settling which may also influence the accuracy of the measured settling velocity.

5. Conclusion

In this article size distribution and settling velocity of granules from a lab scale reactor and industry were studied and the following conclusions were made:

- The shape factor and equivalent diameter used in this article are demonstrated to be a good way to quantify size distribution and settling velocity of granules from lab scale reactors and industries.
- Size and shape of UASB granules vary across a reactor height. Both size and shape factor increases from top section to bottom section of a reactor.
- Settling velocity of UASB granules depend not only on their size and density but also on the shape factor of the granules.

Acknowledgement

This work is part of a PhD project supported by Interreg Biogas2020 in collaboration with University of South-Eastern Norway. The authors would like to thank M.*Sc*. Samee Maharjan for helping with image analysis.

References

Ahn, Y.-H., Speece, R.E., 2003. Settleability assessment protocol for anaerobic granular sludge and its application. Water SA 29 (4), 419–426.
Alpenaar, A., granular Sludge, A., 1994. Characterization and Factors Affecting Its Functioning. PhD thesis, PhD Thesis. Wageningen University, The Netherlands.
Alves, M., Cavaleiro, A.J., Ferreira, E.C., Amaral, A.L., Mota, M., da Motta, M., Vivier, H., Pons, M.-N., 2000. Characterisation by image analysis of anaerobic sludge under shock conditions. Water Sci. Technol. 41 (12), 207–214.
Arsenijević, Z.L., Grbavčić, Ž., Garić-Grulović, R., Bošković-Vragolović, N., 2010. Wall effects on the velocities of a single sphere settling in a stagnant and counter-current fluid and rising in a co-current fluid. Powder Technol. 203 (2), 237–242.
Ataide, C., Pereira, F., Barrozo, M., 1999. Wall effects on the terminal velocity of spherical particles in newtonian and non-newtonian fluids. Braz. J. Chem. Eng. 16 (4), 387–394. http://www.scielo.br/scielo.php?script=sci_arttext&pid=S0104-66321999000400007.
Bellouti, M., Alves, M., Novais, J., Mota, M., 1997. Flocs vs granules: differentiation by fractal dimension. Water Res. 31 (5), 1227–1231.
Bouwman, A.M., Bosma, J.C., Vonk, P., Wesselingh, J.H.A., Frijlink, H.W., 2004. Which shape factor (s) best describe granules? Powder Technol. 146 (1), 66–72.
Chhabra, R., Agarwal, S., Chaudhary, K., 2003. A note on wall effect on the terminal falling velocity of a sphere in quiescent newtonian media in cylindrical tubes. Powder Technol. 129 (1), 53–58.
Dietrich, W.E., 1982. Settling velocity of natural particles. Water Resour. Res. 18 (6), 1615–1626.
Dinamarca, C., Bakke, R., 2009. Apparent hydrogen consumption in acid reactors: observations and implications. Water Sci. Technol. 59 (7), 1441–1447.
Ghangrekar, M., Asolekar, S., Joshi, S., 2005. Characteristics of sludge developed under different loading conditions during uasb reactor start-up and granulation. Water Res. 39 (6), 1123–1133.
Grotenhuis, J., Kissel, J.C., Plugge, C., Stams, A., Zehnder, A., 1991. Role of substrate concentration in particle size distribution of methanogenic granular sludge in uasb reactors. Water Res. 25 (1), 21–27.
Gupta, S.K., Gupta, S., 2005. Morphological study of the granules in uasb and hybrid reactors. Clean Techn. Environ. Policy 7 (3), 203–212.
Laguna, A., Ouattara, A., Gonzalez, R., Baron, O., Fama, G., El Mamouni, R., Guiot, S., Monroy, O., Macarie, H., 1999. A simple and low cost technique for determining the granulometry of upflow anaerobic sludge blanket reactor sludge. Water Sci. Technol. 40 (8), 1–8.
Liu, Y.-h., He, Y.-l., Yang, S.-c., Li, Y.-z., 2006. The settling characteristics and mean settling velocity of granular sludge in upflow anaerobic sludge blanket (uasb)-like reactors. Biotechnol. Lett. 28 (20), 1673–1678.
Mahling, A., 1965. Die dichte. In: Analytik der Lebensmittel, pages 14–40. Springer. https://link.springer.com/chapter/10.1007%2F978-3-662-31684-9_2.
Moy, B.-P., Tay, J.-H., Toh, S.-K., Liu, Y., Tay, S.-L., 2002. High organic loading influences the physical characteristics of aerobic sludge granules. Lett. Appl. Microbiol. 34 (6), 407–412.
Olson, E., 2011. Particle shape factors and their use in image analysis-part 1: theory. J. GXP Compliance 15 (3), 85.
Pereboom, J., 1997. Strength characterisation of microbial granules. Water Sci. Technol. 36 (6–7), 141–148.
Podczeck, F., Newton, J., 1995. The evaluation of a three-dimensional shape factor for the quantitative assessment of the sphericity and surface roughness of pellets. Int. J. Pharm. 124 (2), 253–259.
Pol, L.H., 1989. The Phenomenon of Granulation of Anaerobic Sludge. PhD thesis. Hulshoff Pol.
Pol, L.H., de Castro Lopes, S., Lettinga, G., Lens, P., 2004. Anaerobic sludge granulation. Water Res. 38 (6), 1376–1389.
Tang, C.-J., Zheng, P., Wang, C.-H., Mahmood, Q., Zhang, J.-Q., Chen, X.-G., Zhang, L., Chen, J.-W., 2011. Performance of high-loaded anammox uasb reactors containing granular sludge. Water Res. 45 (1), 135–144.
Thaveesri, J., Daffonchio, D., Liessens, B., Verstraete, W., 1995. Different types of sludge granules in uasb reactors treating acidified wastewaters. Antonie Van Leeuwenhoek

68 (4), 329–337.
Vlyssides, A., Barampouti, E., Mai, S., 2008. Simple Estimation of Granule Size Distribution and Sludge Bed Porosity in a uasb Reactor. a a. 2(1). pp. 4.
Wu, J., Afridi, Z.U.R., Cao, Z.P., Zhang, Z.L., Poncin, S., Li, H.Z., Zuo, J.E., Wang, K.J., 2016. Size effect of anaerobic granular sludge on biogas production: a micro scale study. Bioresour. Technol. 202, 165–171.
Yan, Y.-G., Tay, J.-H., 1997. Characterisation of the granulation process during uasb start-up. Water Res. 31 (7), 1573–1580.
Zhang, G.-D., Li, M.-Z., Xue, J.-Q., Wang, L., Tian, J.-L., 2016. Wall-retardation effects on particles settling through non-newtonian fluids in parallel plates. Chem. Pap. 70 (10), 1389–1398.